Nanoscale Advances

ROYAL SOCIETY OF CHEMISTRY

PAPER

View Article Online
View Journal | View Issue

Cite this: *Nanoscale Adv.*, 2025, **7**, 5993

Immature cotton fibers upcycled into advanced natural nanoparticle synthesizers

Sunghyun Nam, *[a] Shaida S. Rumi,[b] Noureddine Abidi,[b] Hee Jin Kim,[a] Zhongqi He,[c] Doug J. Hinchliffe,[a] Md Nayeem Hasan Kashem,[a] Matthew B. Hillyer[a] and Holly King[d]

As a key agricultural commodity, cotton fibers play a vital role in the global economy. However, unpredictable growing conditions often result in immature cotton fibers, leading to substantial economic losses for both cotton growers and industries. This study revealed the untapped commercial potential of immature cotton fibers—their superior ability to synthesize antimicrobial silver nanoparticles (Ag NPs). Without external reducing or stabilizing agents, immature cotton fibers produced Ag NPs (*ca.* 10 nm in diameter) at a concentration (2 wt% based on the dry fiber weight) more than three times higher than that of mature cotton fibers. This enhanced nanoparticle synthesis was attributed to structural and morphological characteristics of immature cotton fibers, which are defects in traditional textile applications. High Volume Instrument (HVI), Advanced Fiber Information system (AFIS), and fiber cross-sectional analysis showed that immature cotton fibers have a greater surface area for the infusion of Ag precursor ions and higher concentrations of natural reducing agents per unit weight due to their smaller amounts of secondary cell walls and larger amounts of primary cell walls and lumens. The resulting Ag NP-filled fibers are expected to open new market opportunities in filtration systems and biomedical applications.

Received 25th February 2025
Accepted 5th July 2025

DOI: 10.1039/d5na00188a

rsc.li/nanoscale-advances

1. Introduction

The rapid advancements in nanotechnology, which involve the production and application of nanosized materials, have significantly transformed various industries, including the textile industry.[1] In the textile industry, nanotechnology has opened new possibilities for creating innovative functionalities and improving existing performance.[2] For instance, nano-finishing by applying metallic nanoparticles (NPs) such as silver,[3] copper oxide,[4] and zinc oxide NPs,[5] onto textile surfaces can impart antimicrobial activity, coloration, UV protection, self-cleaning capabilities, *etc.* These functionalities are largely attributed to the exceptionally high surface area-to-volume ratio of NPs, which enhances their interaction with surrounding substances, along with their distinctive physical and chemical characteristics.[6] Consequently, the development of efficient, sustainable, and cost-effective methods for the synthesis and application of NPs is essential to fully harnessing nanotechnology's potential in the textile industry.

Conventional chemical synthesis methods for metallic NPs involve a series of steps, including reduction reactions, nucleation, and particle growth.[7] In these methods, a metal precursor (such as a metal salt) is reduced to form metallic atoms, which initiate nucleation by aggregating into nanoclusters. As nucleation progresses, additional metal atoms join the clusters, resulting in the growth of NPs. However, NPs typically aggregate, which negates their desired properties associated with the nanoscopic dimension. The conventional methods, therefore, require the use of chemical agents such as reducing and stabilizing agents. Common reducing agents, including hydrazine, sodium borohydride, and *N*,*N*-dimethylformamide, are effective but pose environmental and health risks due to their toxicity.[8–10] Stabilizing agents—which are necessarily introduced to cap the NPs to prevent uncontrolled aggregation—such as surfactants and polymers are also harmful.[11] It has been reported that the contaminants of these chemical agents could be the source of toxicity to human health rather than the nanoparticles themselves.[12]

This study aims to explore the potential of immature cotton fibers as reagent-free, effective, and economic NP producers. Immature cotton fibers, considered low-quality cotton fibers, are characterized by their short lengths, weak strength,

[a]*Cotton Fiber Bioscience and Utilization Research Unit, U.S. Department of Agriculture, Agricultural Research Service, Southern Regional Research Center, New Orleans, LA 70124, USA. E-mail: sunghyun.nam@usda.gov; Tel: +1-5042864229*

[b]*Department of Plant and Soil Science, Fiber and Biopolymer Research Institute, Texas Tech University, Lubbock, TX 79409, USA*

[c]*Commodity Utilization Research Unit, U.S. Department of Agriculture, Agricultural Research Service, Southern Regional Research Center, New Orleans, LA 70124, USA*

[d]*Cotton Quality and Innovation Research Unit, U.S. Department of Agriculture, Agricultural Research Service, Southern Regional Research Center, New Orleans, LA 70124, USA*

coarseness, and lack of uniformity. The quality of cotton fibers plays a crucial role in the cotton industry, which has an estimated annual global economic impact of over $600 billion.[13,14] High-quality cotton fibers with desirable traits such as length, strength, fineness, maturity, and uniformity are required in the market. However, immature cotton fibers often result from various factors, including weather patterns, water availability, soil conditions, nutrient levels, and disease. The increasing frequency and severity of adverse weather events, such as rising temperatures and reduced rainfall during the cotton-growing season, are expected to increase the production of immature, low-quality cotton fibers.[15,16] For example, environmental stresses during cotton fiber development and maturation have been reported to disrupt fiber elongation, reducing fiber length[17] and interfering with cellulose synthesis in the secondary cell wall, which compromises the structural integrity of the fibers.[18]

Poor fiber quality leads to processing difficulties and is penalized with price reductions, resulting in financial losses for cotton growers and industries.[19,20] Since immature cotton fibers do not meet the quality standards required for traditional textile applications, such as yarn spinning and fabric production, they are usually used in lower-grade nonwoven applications. With the rising consumption and demand for cotton fibers,[21] coupled with increasingly unpredictable weather patterns,[15,16] the production of immature cotton fibers is expected to grow. Therefore, developing innovative methods to upcycle immature cotton fibers is crucial. Some efforts have been made to convert low-quality cotton fibers into value-added products, such as bioplastics,[22] mulch gel films,[23] cellulose films,[24] and conductive biomaterials.[25]

In this study, we transformed immature cotton fibers into an efficient biosynthesizer for generating antimicrobial silver nanoparticles (Ag NPs) by leveraging their structural and morphological characteristics, which are typically detrimental to conventional textile applications. The specific objectives of this study are to: (1) analyze the structural and morphological distinctions of immature cotton fibers; (2) understand how these structural and morphological defects enhance synthetic efficiency; and (3) demonstrate the production of Ag NPs using immature cotton fibers and characterize the resulting Ag NPs. The Ag NP-filled immature cotton fibers produced in this study have the potential to open new markets in filtration systems, biomedical applications, and advanced composites. By creating new commercial pathways for immature, low-quality cotton fibers—traditionally sold at low prices—this approach could add value to these fibers and help increase revenue for cotton growers and the cotton manufacturing industry.

2. Experimental

2.1. Materials

Immature cotton fibers were obtained from the Fiber and Biopolymer Research Institute at Texas Tech University, Lubbock, TX, and universal standard cotton fibers for micronaire calibration (Au-35434) were obtained from the USDA AMS Cotton and Tobacco Program, Memphis, TN. Silver nitrate ($AgNO_3$, 99.9%) was purchased from J. T. Baker (Radnor, PA, USA), and methyl methacrylate, butyl methacrylate, benzoyl peroxide, ethanol, and nitric acid (HNO_3, 70%, Trace Metal Grade) were purchased from Sigma-Aldrich (St. Louis, MO, USA). All chemicals were used as received without further purification. Deionized (DI) water was used as a solvent.

2.2. Synthesis of Ag nanoparticles by cotton fibers

Approximately 0.2g of cotton fibers were placed in a 100 mL round-bottom flask, and 15 mL of an aqueous 0.01 M $AgNO_3$ solution was added. The fibers were gently tapped and pressed using a stainless-steel spatula to ensure a complete submersion in the solution. The submerged fibers were left to react at room temperature for 24 h. Following this, a water condenser was connected to the flask, which was then placed in an oil bath and heated to 100 °C for 1 h. During this synthetic process, the samples were periodically removed, placed in vials, and photographed to record any color changes. After the treatment, the fibers were washed with ethanol and then with DI water multiple times to remove unreacted $AgNO_3$ and air-dried at room temperature.

2.3. Characterization

2.3.1. Image analysis. Photographs of the samples were taken using a digital camera (RX100, Sony, San Diego, CA). Optical microscopic images of cotton fibers were acquired in reflection mode for longitudinal views and in transmission mode for cross-sectional views using a digital microscope (KH-8700, Hirox, Oradell, NJ). To prepare fiber cross-sections, cotton fibers were embedded in a mixture of methyl methacrylate, butyl methacrylate, and benzoyl peroxide. Following published protocols,[26,27] this mixture was polymerized for 30 min using a UV cross-linker (UVP CL-1000, Analytik, Jena, Germany). The polymerized blocks were sliced into sections approximately 1 μm thick using a microtome (PowerTome Ultramicrotome, Boeckeler Instruments, Tucson, AZ). These thin sections were then placed on glass slides for imaging.

The cross-sectional images of the fibers were further analyzed using Fibre Image Analysis Software-2 (FIAS-2) according to previously described methods.[28,29] Parameters such as cross-sectional fiber area, cross-sectional fiber perimeter, cross-sectional lumen area, and cross-sectional lumen perimeter were obtained. Averages for these parameters were determined from approximately 100 fiber cross-sections per sample.

TEM images and selected area electron diffraction (SAED) patterns were acquired using a TEM (JEM-2011, Jeol, Peabody, MA) operating at 200 kV. Samples were prepared using the same protocol as the fiber cross-sections for optical microscopy, except that the polymerized blocks were sliced into sections approximately 100 nm thick. These sections were placed onto carbon-film-coated copper grids. The size of Ag NPs was measured by analyzing TEM micrographs using Image-J software.[30]

2.3.2. Spectral analysis. Ultraviolet-visible (UV-vis) spectra were collected using a UV-vis spectrophotometer (ISR-2600, Shimadzu, Columbia, MD) equipped with an integrating sphere unit. Both diffuse reflectance and absorbance spectra

were measured over a wavelength range of 200–1200 nm. Reflectance spectra in the visible range (380–780 nm) were used to calculate the CIE LAB color coordinates (L^*, a^*, and b^*) using the UV-2401PC Color Analysis software. The parameter L^* represents lightness, where a value of 0 corresponds to black and 100 to white. The parameter a^* represents the red-green axis, with negative values indicating green and positive values indicating red, while b^* represents the yellow–blue axis, where negative values indicate blue and positive values indicate yellow. The color difference (ΔE^*) was calculated using the equation:

$$\Delta E^* = \sqrt{(\Delta L)^2 + (\Delta a)^2 + (\Delta b)^2} \quad (1)$$

where ΔL, Δa, and Δb are the differences in the L^*, a^*, and b^* values, respectively. The reported ΔE^* value represents the average of five measurements.

2.3.3. Fiber property measurement. The micronaire and maturity index of cotton fibers were measured from fiber bundles using a High Volume Instrument (HVI) test with the USTER® HVI 1000 (USTER Technologies Inc., Knoxville, TN). Prior to testing, the fibers were conditioned for 48 h at 21 ± 1 °C and 65 ± 2% relative humidity. The instrument was calibrated using standard cotton fibers provided by the USDA Agricultural Marketing Service. The average values of the parameters were calculated from five individual measurements per sample.

The maturity ratio and fineness of the cotton fibers were measured from individualized fibers using an Advanced Fiber Information System (AFIS) test with the AFIS PRO 2 (USTER Technologies Inc., Knoxville, TN). Fibers were conditioned under the same environment (21 ± 1 °C and 65 ± 2% relative humidity for 48 h) before testing. A fiber strand (sliver) was directed into an accelerated airstream and analyzed using

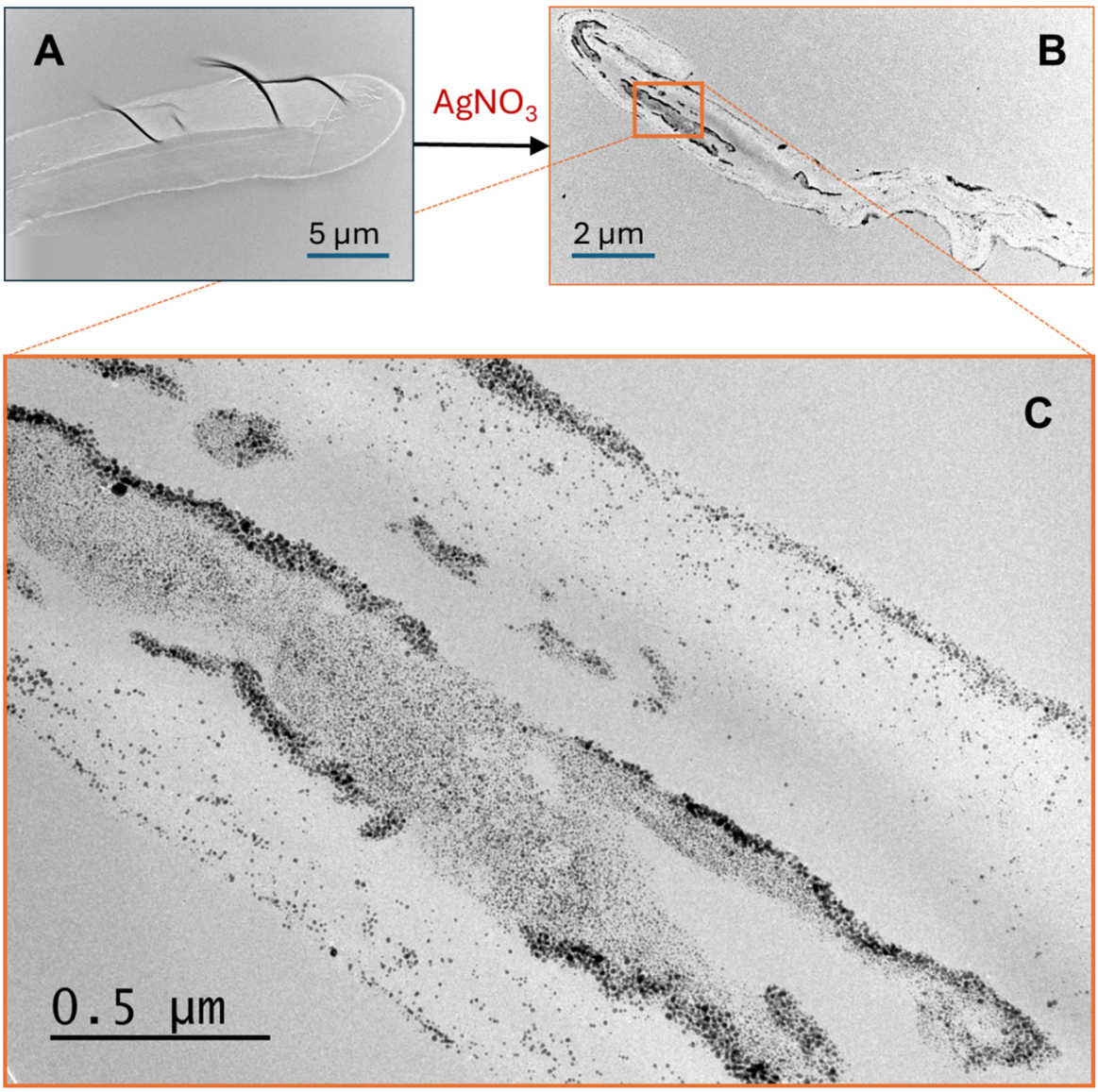

Fig. 1 TEM images of immature cotton fibers (A) before and (B) after the treatment with $AgNO_3$ at low magnification. (C) Higher-magnification TEM image of the region marked by the red rectangle in (B).

electro-optical sensors. For each sliver, 5000 individualized fibers were measured. The average values of the parameters were calculated from five slivers.

2.3.4. Ag element analysis. The Ag content in the cotton fibers was quantified using a graphite furnace atomic absorption spectrometer (240Z AA, Agilent, Santa Clara, CA). For sample preparation, approximately 0.1 g of cotton fibers were digested with 10 mL of 6 M trace-metal-grade nitric acid using a microwave digestion system (MARS 6, CEM Corporation, Matthews, NC). The resulting solution was diluted 1 : 1000 (by weight) and analyzed based on an external calibration curve prepared with an Ag single-element standard (Agilent, Santa Clara, CA). The reported Ag concentration is the average of three measurements.

3. Results and discussion

3.1. Potential function of immature cotton fibers

The conventional chemical synthesis of metallic NPs typically involves the use of reducing agents to convert metal ions into zero-valent metal atoms and stabilizing agents to regulate particle growth and prevent NP aggregation. However, previous studies have demonstrated that raw cotton fibers (not scoured and bleached) can induce the synthesis of Ag NPs without requiring external reducing and stabilizing agents.[3,31–34] This intrinsic capability is attributed to the unique structure and chemical composition of the fibers. In this study, we hypothesized that immature cotton fibers could induce high-yield nanoparticle production due to their distinctive structural and morphological characteristics. Fig. 1A and B show TEM images of immature cotton fiber cross-sections before and after $AgNO_3$ treatment alone, respectively, at low magnification. The treated fibers exhibited noticeable dark spots along their edges and center, indicating the deposition of a high concentration of Ag. A magnified view (Fig. 1C) revealed the formation of numerous Ag NPs, with a greater number and more extensive distribution compared to those in previous studies.[3,31–34]

3.2. Structure and morphology of immature cotton fibers

To investigate the Ag NP synthetic capacity of immature, low-quality cotton fibers, their structural and morphological

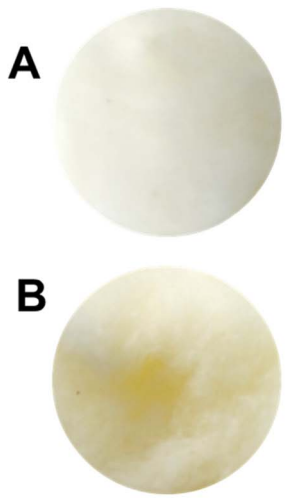

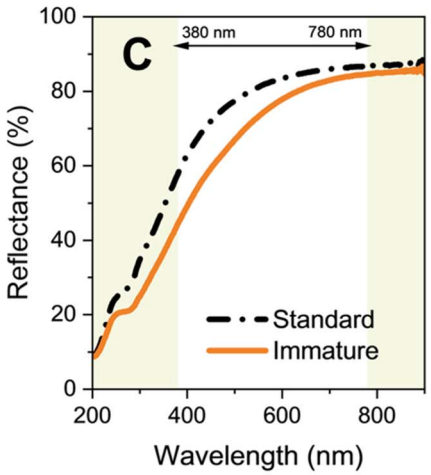

D

	Standard	Immature
L^*	89.58 (1.59)	87.56 (2.57)
a^*	-0.41 (0.09)	0.35 (0.26)
b^*	5.94 (0.46)	11.62 (0.57)

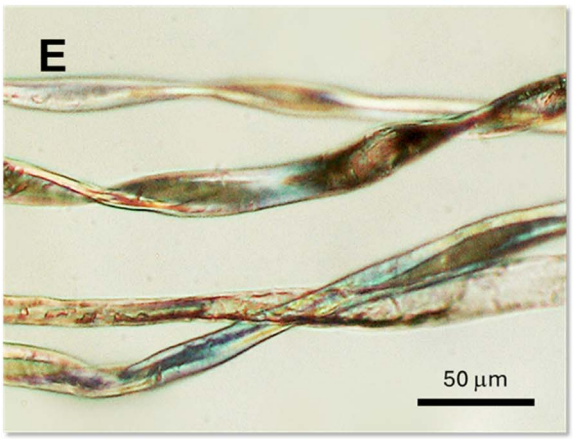

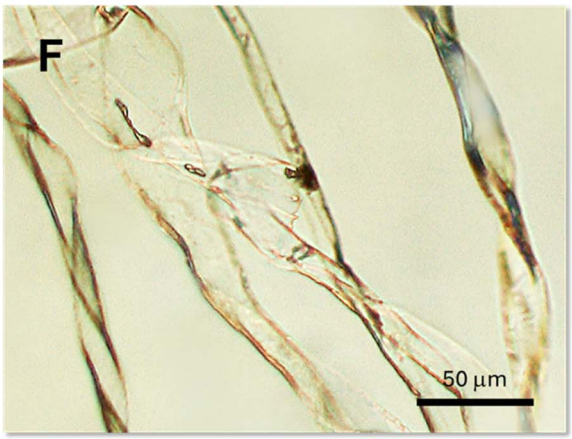

Fig. 2 Photographs of (A) standard and (B) immature cotton fibers. (C) UV-vis reflectance spectra and (D) CIE LAB color coordinates of standard and immature cotton fibers. The visible light range (380–780 nm) used to calculate color coordinates was indicated in white. Numbers in parentheses are standard deviations. Optical microscopic images of the longitudinal views of (E) standard and (F) immature cotton fibers obtained in reflection mode.

characteristics were compared with those of standard cotton fibers that are used in fiber quality tests. Visually, immature cotton fibers appeared noticeably yellower than standard cotton fibers (Fig. 2A and B). Consistently, the UV-vis reflectance spectrum of immature cotton fibers exhibited lower reflectance in the visible light range (380–780 nm) (Fig. 2C). From this reflectance data, the CIE LAB color coordinates were calculated (Fig. 2D). The L^* value of immature cotton fibers was slightly lower than that of standard cotton fibers, indicating reduced lightness. The contrasting a^* values—positive for immature cotton fibers and negative for standard cotton fibers—suggest that immature cotton fibers tend toward red tones, while standard cotton fibers lean toward green. The b^* values further confirmed that immature cotton fibers are more yellow than standard cotton fibers. The calculated ΔE^* value, using eqn (1), was 5.9 ± 1.1, indicating a color difference that is noticeable at a glance.

Raw cotton fibers typically contain small amounts of pigments,[35] which impart a slightly yellow hue. The main component of cotton fiber pigments is different types of flavonoids.[36] The lower reflectance in the UV range for immature cotton fibers suggests relatively higher levels of flavonoids. The characteristic UV absorption of flavonoids consists of two major bands, band I associated with the B-ring cinnamoyl system at 300–380 nm and band II with the A-ring benzoyl system at 240–280 nm.[37] This increased pigment content in immature cotton fibers promotes their Ag NP synthesis, as flavonoids in the pigments[36] can act as reducing agents.[33] The phenolic groups abundant in flavonoids donate electrons to Ag^+ ions in redox reactions, reducing them into Ag^0 atoms.

Fig. 2E and F show optical microscopic images of the longitudinal views of standard and immature cotton fibers, respectively, obtained in reflection mode. The images reveal distinct morphological differences. Standard cotton fibers exhibit a convoluted and flattened structure, characteristic of mature cotton fibers. These twists and flattened features develop as the fibers collapse during the drying process.[35] Immature cotton fibers appear more flattened with fewer convolutions and show greater variability in diameter across individual fibers, reflecting their less uniform and incomplete development. Notably, immature cotton fibers appear more transparent under the optical microscope than standard cotton fibers. This increased transparency suggests that immature cotton fibers have thinner cell walls and larger lumens. Lumens are the hollow canals at the center of the fibers. These structural distinctions are further supported by cross-sectional views of standard and immature cotton fibers (Fig. 3). Standard cotton fibers show bean-shaped cross-sections with relatively thicker

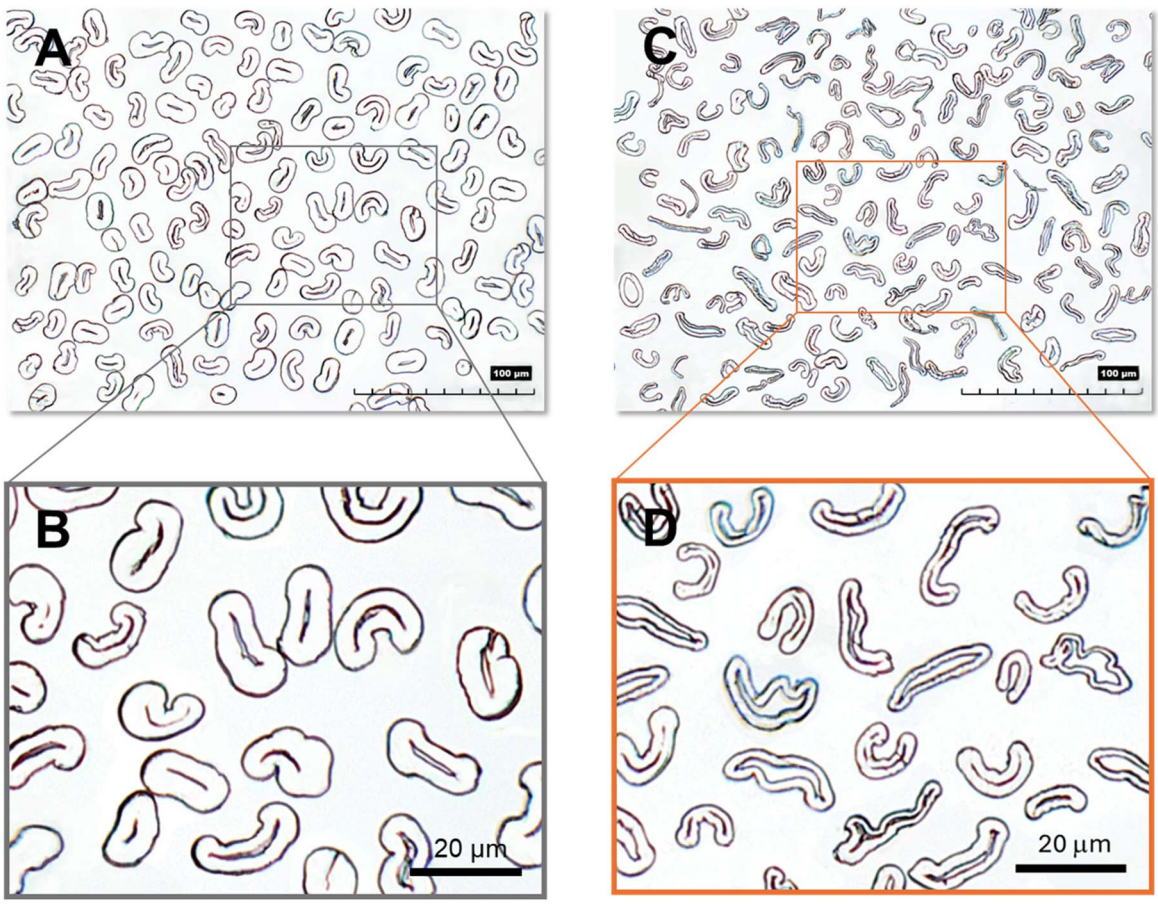

Fig. 3 Optical microscopic images of the cross-sectional views of standard cotton fibers at (A) low and (B) high magnifications and immature cotton fibers at (C) low and (D) high magnifications.

cell walls and smaller lumens. In contrast, immature cotton fibers exhibit a worm-like cross-section characterized by a collapsed, elongated, and irregular appearance. Consistent with their transparency in the longitudinal view, immature cotton fibers have thinner cell walls and wider, larger lumens.

The structural and morphological differences between standard and immature cotton fibers were quantified using HVI and AFIS tests. Fig. 4 presents the selected parameters measured from these tests. The micronaire, which measures the air permeability of a bundle of fibers as an indicator of fiber maturity and fineness, was 2.2 for immature cotton fibers—approximately 60% lower than that of standard cotton fibers (Fig. 4A). Similarly, the maturity index of immature cotton fibers was about 9% lower than that of standard cotton fibers (Fig. 4B). Both parameters fell below the critical thresholds for classifying mature cotton fibers—3.5 for micronaire and 0.85 for maturity index—confirming that the fibers are immature. Since immature cotton fibers adversely affect textile processing, they are considered unsuitable for traditional textile applications such as spinning yarns and manufacturing fabrics.[38] Consistent with the microscopic observations, the fineness of immature cotton fibers was about 25% lower than that of standard cotton fibers (Fig. 4C and D). Although the variation in fineness was similar between the two fibers, the fineness distribution of immature cotton fibers was left-skewed, reflecting a greater proportion of finer fibers. In terms of fiber length, immature cotton fibers were approximately 18% shorter than standard cotton fibers (Fig. 4E and F). The shorter fiber length, combined with the greater fineness of immature cotton fibers, offers an additional advantage for Ag NP synthesis—an increased surface area for the infusion of Ag precursor ions compared to standard cotton fibers of the same weight.

Fig. 5 shows the results of the quantitative analysis of standard and immature cotton fiber cross-sections. Using Fibre

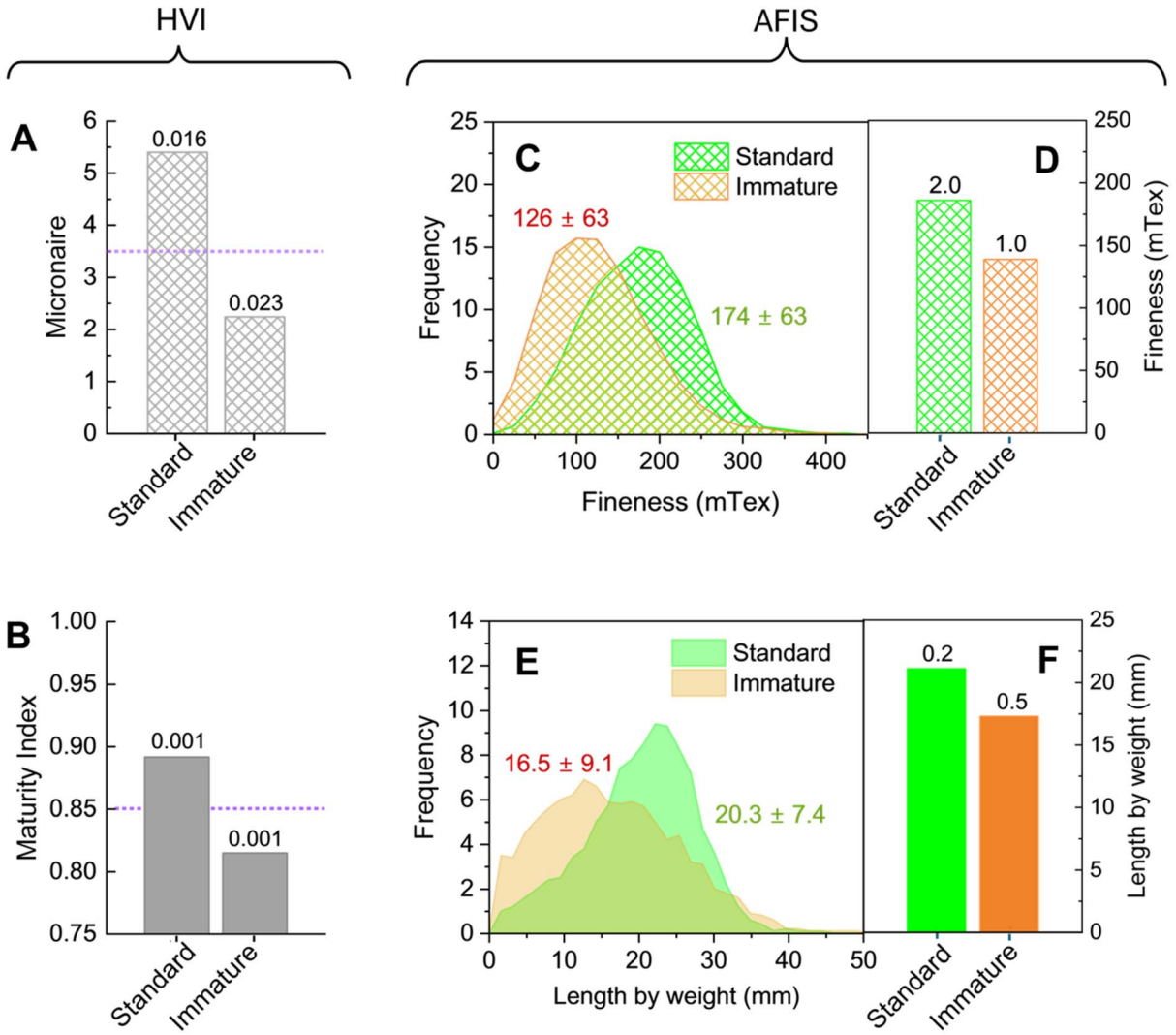

Fig. 4 (A) Micronaire and (B) maturity index of standard and immature cotton fibers measured using HVI testing. Purple dotted lines indicate critical thresholds for classifying mature cotton fibers. (C) Distributions and (D) average values of maturity ratios and (E) distributions and (F) average values of fineness for standard and immature cotton fibers measured using AFIS testing. The numbers placed on the top of bars represent standard deviations.

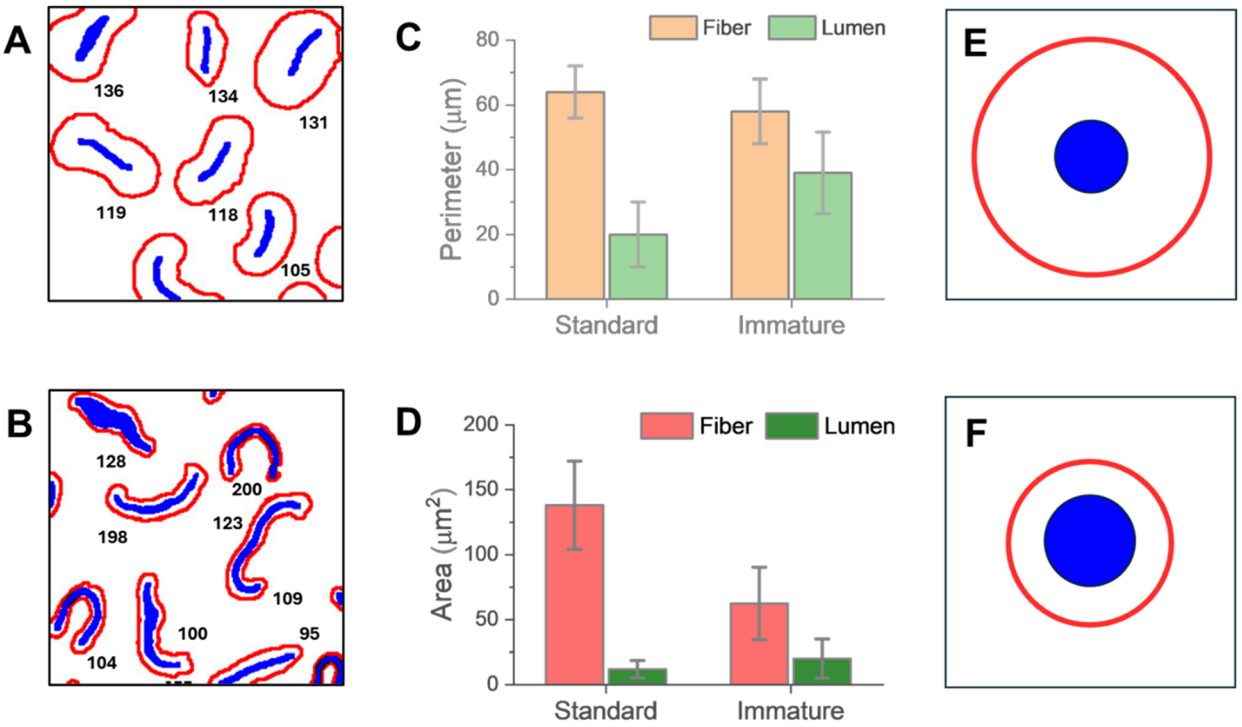

Fig. 5 Representative microscopic image analyses of the cross sections of (A) standard and (B) immature cotton fibers. (C) Perimeters and (D) areas of fiber excluding the lumen area and lumen for standard and immature cotton fibers. Idealized cross-sectional diagrams of single fibers for (E) standard and (F) immature cotton fibers constructed based on the measured areas. The blue regions represent lumen areas, and the red solid lines represent fiber perimeters.

Image Analysis Software, the perimeters and areas of fibers and lumens were measured for approximately 100 fibers. Representative cross-sectional images of standard and immature cotton fibers are shown in Fig. 5A and B, respectively. The fiber perimeter of immature cotton fibers was slightly smaller (about 9% less) than that of standard cotton fibers; however, the lumen perimeter of immature cotton fibers was nearly twice as large as that of standard cotton fibers (Fig. 5C). The cross-sectional fiber area of immature cotton fibers was less than half that of standard cotton fibers (Fig. 5D), whereas the cross-sectional lumen area of immature cotton fibers was approximately 67% larger. To visually compare the cross-sectional morphology, idealized diagrams of single fibers for standard and immature cotton fibers were constructed based on their measured areas (Fig. 5E and F, respectively). These diagrams highlight that, for the same weight, immature cotton fibers have a larger proportion of the primary cell wall (outer layer) and lumen but a smaller portion of the secondary cell wall (inner layer comprising most of the cotton fiber) compared to standard cotton fibers. The primary cell wall and lumen contain most of the non-cellulosic components with reducing properties, such as pectin, sugars, nuclei, protoplasm, and other metabolic byproducts.[35,39] In contrast, the secondary cell wall is primarily composed of cellulose with a limited number of reactive hydroxyl chain end groups. Therefore, it can be concluded that, at an equal weight, immature cotton fibers contain a higher concentration of natural reducing agents, and their larger lumens—hollow canals running the length of the fiber—facilitate the infusion of Ag precursor ions into the fiber, thereby improving their ability to synthesize Ag NPs.

3.3. Immature cotton fiber-induced synthesis of Ag NPs

To evaluate the effectiveness of immature cotton fibers to induce Ag NP synthesis, standard and immature cotton fibers were treated with $AgNO_3$ without the addition of external reducing or stabilizing agents. Fig. 6 shows photographs of standard and immature cotton fibers during the treatment process. Both standard and immature cotton fibers gradually turned brown upon immersion in the aqueous $AgNO_3$ solution at room temperature. This coloration is a visual indication of Ag NP formation attributed to their unique optical properties. Even at room temperature, naturally occurring reducing agents in raw cotton fibers facilitated the reduction of Ag^+ ions to Ag^0 atoms. As the immersion time increased, the fibers' colors darkened progressively, with immature cotton fibers exhibiting more rapid and pronounced darkening compared to standard cotton fibers. After 24 h, immature cotton fibers exhibited a vibrant brown hue. Subsequent heat treatment at 100 °C for 1 h further intensified the coloration, turning both standard and immature cotton fibers dark drown. Immature cotton fibers remained darker than standard cotton fibers.

To quantitatively analyze Ag NP formation, surface plasmon resonance (SPR) intensities of treated standard cotton and immature cotton fibers were measured using UV-vis spectroscopy (Fig. 7A). SPR arises when conduction electrons on the

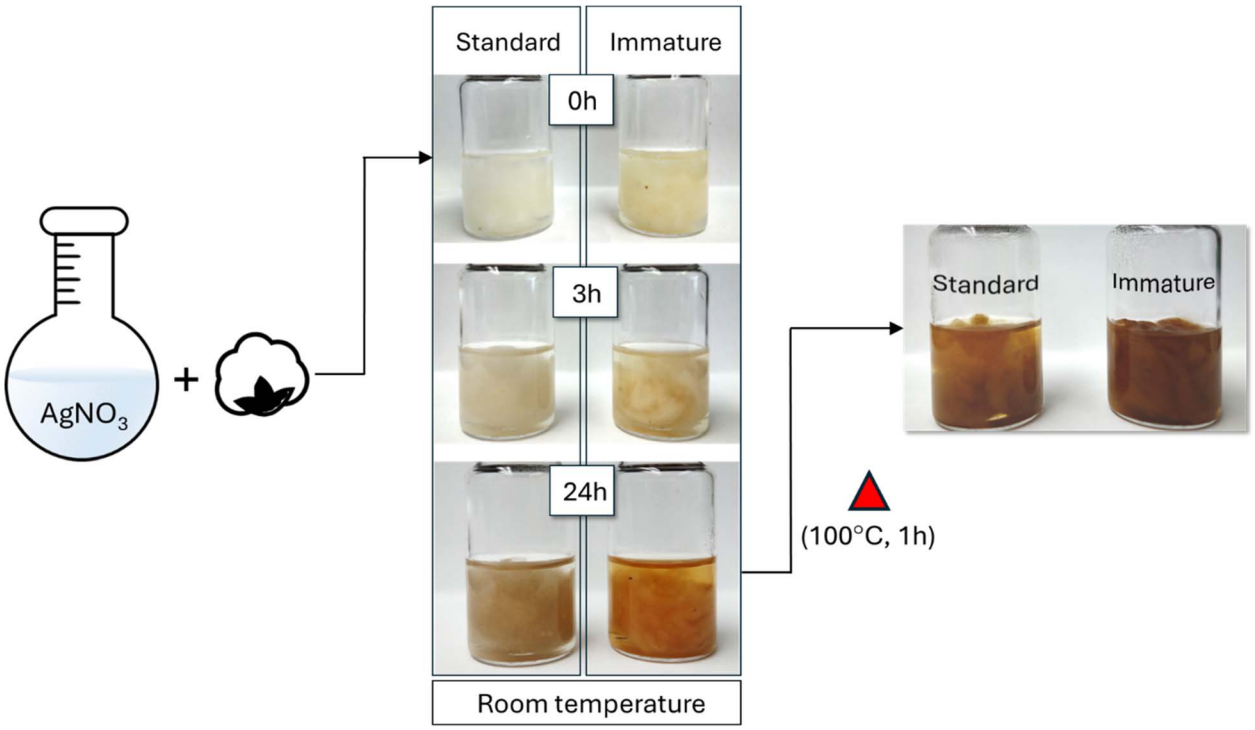

Fig. 6 *In situ* cotton fiber-induced synthesis of Ag NPs: photographs of standard and immature cotton fibers in aqueous $AgNO_3$ solutions at different time intervals at room temperature and after subsequent heat treatment.

surface of metallic NPs resonate with incident light at specific wavelengths, producing distinctive absorption peaks.[40] The intensity of these peaks correlates with the concentration of NPs, as a higher number of NPs amplifies the collective oscillation of conduction electrons. Both standard and immature cotton fibers exhibited strong, sharp SPR peaks centered at approximately 430 nm, consistent with the characteristic SPR of Ag NPs. However, the SPR intensity of immature cotton fibers was 32% higher than that of standard cotton fibers. Further analysis of the Ag concentration, based on the dry weight of fibers, revealed that immature cotton fibers contained 1.92 wt% Ag, compared to 0.61 wt% Ag for standard cotton fibers (Fig. 7B). These findings demonstrate that immature cotton fibers exhibit a superior Ag NP synthesis capacity, producing over three times the Ag NP yield of standard cotton fibers.

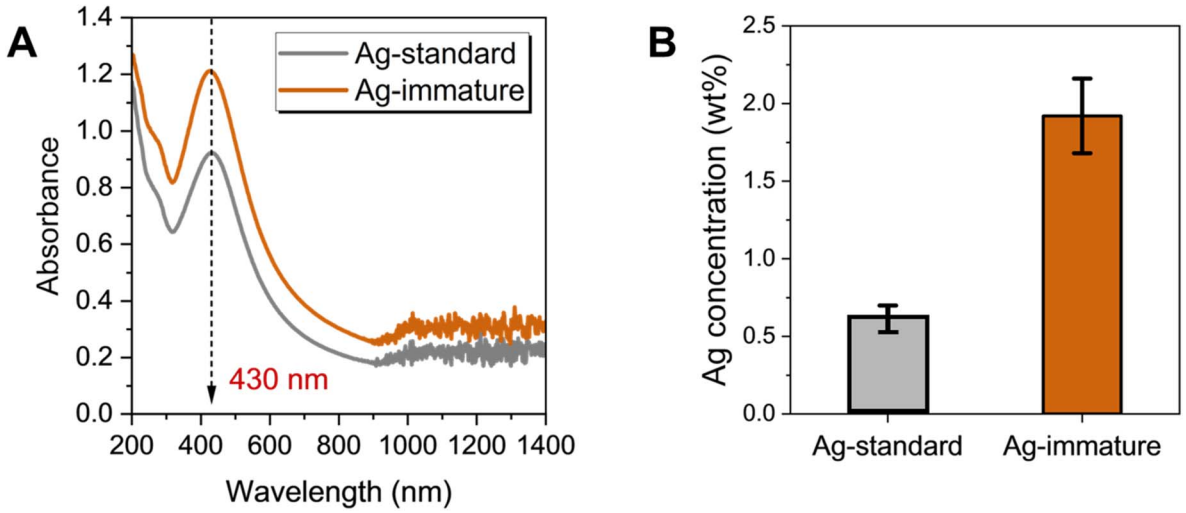

Fig. 7 (A) UV-vis absorbance spectra of Ag NP-filled standard cotton fibers (Ag-standard) and Ag NP-filled immature cotton fibers (Ag-immature). Their surface plasmon resonance peak wavelength was labeled. (B) Ag concentrations in Ag-standard and Ag-immature cotton fibers measured based on their dry weights.

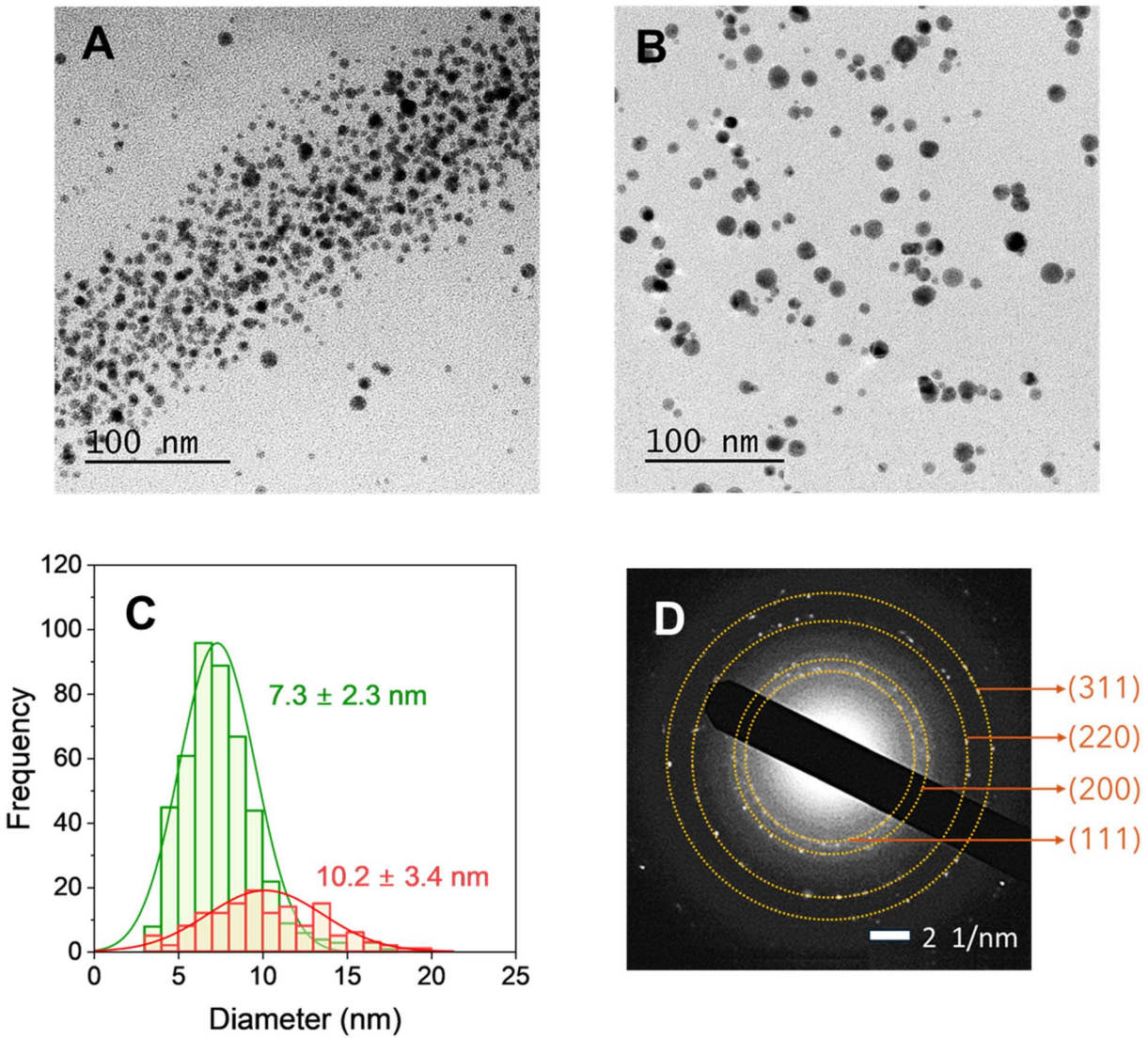

Fig. 8 TEM images of Ag NPs formed in the (A) lumen and (B) primary cell wall of immature cotton fibers. (C) Histograms of Ag NP size distributions in the lumen and primary cell wall of immature cotton fibers, with Gaussian fits represented by solid lines. (D) SAED pattern of Ag NPs in the lumen with diffraction planes of Ag labeled on the concentric rings.

Fig. 8A and B show TEM images of Ag NPs formed in the lumen and primary cell wall of immature cotton fibers, respectively. Higher populations of NPs were observed in the lumen and primary cell wall than in the secondary cell wall (Fig. 1). The lumen, originally filled with living protoplasts during fiber growth, dries up as the fiber matures, leaving behind protoplast remnants, cell nuclei, and other metabolic byproducts. The primary cell wall also contains various non-cellulosic components, including sugars, pectin, proteins, and pigments. These non-cellulosic components can serve as natural reducing agents. The reducing capability of these natural components has been validated in a previous study investigating the effects of scouring—a process that removes non-cellulosic materials. That study demonstrated a significant reduction in nanoparticle synthesis following scouring: scoured cotton fibers produced markedly fewer silver nanoparticles compared to raw cotton fibers, with yields of 41 mg kg^{-1} *versus* 2261 mg kg^{-1}, respectively.[32] Within the fiber lumen, the NPs were found to be densely concentrated yet remained individually dispersed without aggregation, indicating the cotton fiber matrix as an effective and stable platform for nanoparticle stabilization.

Based on the TEM images of Ag NPs in the lumen and primary cell wall, particle sizes were analyzed and compared. Fig. 8C shows the size distributions in the two regions, which were fitted to Gaussian functions. The size distribution of Ag NPs in the lumen was slightly narrower and shifted toward smaller sizes compared to those in the primary cell wall. The average diameters were determined to be 7.3 ± 2.3 nm for NPs in the lumen and 10.2 ± 3.4 nm in the primary cell wall. The SAED pattern obtained from the NPs in the lumen showed four distinct concentric rings corresponding to the (1 1 1), (2 0 0), (2 2 0), and (3 1 1) planes of a face-centered cubic crystalline

structure of Ag, confirming that the NPs are composed of elemental Ag (Fig. 8D).

Nanoparticles embedded within the interior of cotton fibers offer significant advantages over those treated on the fiber surface. Conventional nanoparticle applications in the textile industry predominantly rely on surface treatments, where nanoparticles are deposited onto the exterior of fibers. However, recent studies have shown that such surface-treated nanoparticles are prone to detachment during laundering, raising both environmental and health concerns.[41–43] To enhance surface adhesion, various strategies such as plasma or corona treatments have been employed to introduce surface roughness and increase binding sites.[44–46] Our approach eliminates the need for modification of fiber surface by enabling *in situ* synthesis of nanoparticles within the fiber's internal structure. This embedded configuration provides superior durability and resistance to nanoparticle leaching.[3,32,33,47,48]

4. Conclusions

Nanotechnology offers transformative solutions across various fields but often relies on complex and expensive chemical processes. This study reported new uses of immature cotton fibers as simple, cost-effective, and reagent-free NP synthesizers, changing their perception from waste material to a valuable resource in sustainable nanotechnology. The structural and morphological defects in immature cotton fibers were found to play critical roles in the effective *in situ* synthesis of Ag NPs. The greater amount of the lumen and the primary cell walls per unit fiber weight served as reservoirs for natural reducing agents, eliminating the need for external chemical agents. The large perimeter and area of lumen, along with the fineness of immature fibers, facilitated the infusion of Ag precursor ions. As a result, compared to standard cotton fibers, immature cotton fibers led to three times higher yield of Ag NPs (*ca.* 10 nm in diameter) individually formed within the fiber. This finding not only provides an alternative, high-value application for immature cotton fibers but also introduces a sustainable method for NP synthesis. The resulting NP-filled cotton fibers have significant potential for integration into advanced materials with promising applications in durable antimicrobial filtration systems and protective healthcare products.

Data availability

The raw data of this study are available from the corresponding author upon request.

Conflicts of interest

The authors declare that the research was conducted in the absence of any commercial or financial relationships that could be construed as a potential conflict of interest.

Acknowledgements

The authors would like to thank the LSU Shared Instrument Facility for their assistance in data collection. USDA is an equal opportunity provider and employer. This research was funded by the USDA-ARS & TTU Collaborative Seed Grant.

References

1 M. A. Shah, B. M. Pirzada, G. Price, A. L. Shibiru and A. Qurashi, Applications of nanotechnology in smart textile industry: a critical review, *J. Adv. Res.*, 2022, **38**, 55–75.
2 M. Syduzzaman, A. Hassan, H. R. Anik, M. Akter and M. R. Islam, Nanotechnology for high-performance textiles: a promising frontier for innovation, *ChemNanoMat*, 2023, **9**, e202300205.
3 S. Nam, D. J. Hinchliffe, M. B. Hillyer, L. Gary and Z. He, Washable Antimicrobial Wipes Fabricated from a Blend of Nanocomposite Raw Cotton Fiber, *Molecules*, 2023, **28**, 1051.
4 M. B. Hillyer, S. Nam and B. D. Condon, Intrafibrillar dispersion of cuprous oxide (Cu_2O) nanoflowers within cotton cellulosic fabrics for permanent antibacterial, antifungal, and antiviral activity, *Molecules*, 2022, **27**, 7706.
5 A. Lawrynowicz, E. Palo, R. Nizamov and K. Miettunen, Self-cleaning and UV-blocking cotton – fabricating effective ZnO structures for photocatalysis, *J. Photochem. Photobiol., A*, 2024, **450**, 115420.
6 J. A. Enterkin, K. R. Poeppelmeier and L. D. Marks, Oriented Catalytic Platinum Nanoparticles on High Surface Area Strontium Titanate Nanocuboids, *Nano Lett.*, 2011, **11**, 993–997.
7 J. Belloni, J.-L. Marignier and M. Mostafavi, Mechanisms of metal nanoparticles nucleation and growth studied by radiolysis, *Radiat. Phys. Chem.*, 2020, **169**, 107952.
8 H. Liu, X. Wang, Y. Wu, J. Hou, S. Zhang, N. Zhou and X. Wang, Toxicity responses of different organs of zebrafish (Danio rerio) to silver nanoparticles with different particle sizes and surface coatings, *Environ. Pollut.*, 2019, **246**, 414–422, DOI: **10.1016/j.envpol.2018.12.034**.
9 L. Yuan, C. J. Richardson, M. Ho, C. W. Willis, B. P. Colman and M. R. Wiesner, Stress Responses of Aquatic Plants to Silver Nanoparticles, *Environ. Sci. Technol.*, 2018, **52**(5), 2558–2565, DOI: **10.1021/acs.est.7b05837**.
10 B. P. Espinasse, N. K. Geitner, A. Schierz, M. Therezien, C. J. Richardson, G. V. Lowry, L. Ferguson and M. R. Wiesner, Comparative Persistence of Engineered Nanoparticles in a Complex Aquatic Ecosystem, *Environ. Sci. Technol.*, 2018, **52**(7), 4072–4078, DOI: **10.1021/acs.est.7b06142**.
11 N. Abramenko, M. Semenova, A. Khina, P. Zherebin, Y. Krutyakov, E. Krysanov and L. Kustov, The toxicity of coated silver nanoparticles and their stabilizers towards paracentrotus lividus sea urchin embryos, *Nanomaterials*, 2022, **12**, 4003.
12 M. E. Samberg, S. J. Oldenburg and N. A. Monteiro-Riviere, Evaluation of silver nanoparticle toxicity in skin *in vivo* and

keratinocytes *in vitro*, *Environ. Health Perspect.*, 2010, **118**(3), 407–413, DOI: 10.1289/ehp.0901398.
13 M. A. Khan, A. Wahid, M. Ahmad, M. T. Tahir, M. Ahmed, S. Ahmad and M. Hasanuzzaman, World cotton production and consumption: an overview, in *Cotton Production and Uses*, ed. Ahmad, S., Hasanuzzaman, M., Springer Singapore, 2020, pp 1–7.
14 D. Tokel, B. N. Genc and I. I. Ozyigit, Economic impacts of Bt (*Bacillus thuringiensis*) cotton, *J. Nat. Fibers*, 2022, **19**, 4622–4639.
15 K. Kothari, S. Ale, J. P. Bordovsky, C. L. Munster, V. P. Singh, J. Nielsen-Gammon and G. Hoogenboom, Potential genotype-based climate change adaptation strategies for sustaining cotton production in the Texas High Plains: a simulation study, *Field Crops Res.*, 2021, **271**, 108261.
16 K. R. Reddy, P. R. Doma, L. O. Mearns, M. Y. L. Boone, H. F. Hodges, A. G. Richardson and V. G. Kakani, Simulating the impacts of climate change on cotton production in the Mississippi Delta, *Climate Research*, 2002, **22**, 271–281.
17 H. Zhu, W. Hu, Y. Li, J. Zou, J. He, Y. Wang, S. Wang and Z. Zhou, Drought shortens cotton fiber length by inhibiting biosynthesis, remodeling and loosening of the primary cell wall, *Ind. Crops Prod.*, 2023, **200**, 116827.
18 W. Hu, M. Gao, B. Xu, S. Wang, Y. Wang and Z. Zhou, Co-occurring elevated temperature and drought stresses during cotton fiber thickening stage inhibit fiber biomass accumulation and cellulose synthesis, *Ind. Crops Prod.*, 2022, **187**, 115348.
19 S. Beegum, V. Reddy and K. R. Reddy, Development of a cotton fiber quality simulation module and its incorporation into cotton crop growth and development model: GOSSYM, *Comput. Electron. Agric.*, 2023, **212**, 108080.
20 J. M. Bradow and G. H. Davidonis, Quantitation of fiber quality and the cotton production-processing interface: a physiologist's perspective, *J. Cotton Sci.*, 2000, **4**, 31.
21 S. MacDonald, K. Lanclos, L. Meyer and G. Soley, *The World and United States Cotton Outlook; USDA's 100th Annual Agricultural Outlook Forum*, 2024.
22 S. S. Rumi, S. Liyanage and N. Abidi, Conversion of low-quality cotton to bioplastics, *Cellulose*, 2021, **28**, 2021–2038.
23 S. S. Rumi, S. Liyanage, Z. Zhang and N. Abidi, Upcycling low-quality cotton fibers into mulch gel films in a fast closed carbon, *Gels*, 2024, **10**, 218.
24 S. S. Rumi, S. Liyanage and N. Abidi, Soil burial-induced degradation of cellulose films in a mositure-controlled envrionment, *Sci. Rep.*, 2024, **14**, 6921.
25 S. Demirci, M. Sahiner, S. S. Rumi, S. S. Suner, N. Abidi and N. Sahiner, The use of low-quality cotton-derived cellulose films as templates for in situ conductive polymer synthesis as promising biomaterials in biomedical applications, *Macromol. Mater. Eng.*, 2025, **310**, 2400246.
26 D. P. Thibodeaux and J. P. Evans, Cotton fiber maturity by image analysis, *Text. Res. J.*, 1986, **56**, 130–139.
27 E. K. Boylston, O. Hinojosa and J. J. Hebert, A quick embedding method for light and electron microscopy of textile fibers, *Biotech. Histochem.*, 1991, **66**(3), 122–124.
28 B. Xu and Y. Huang, Image analysis for cotton fibers Part II: Cross-sectional measurements, *Text. Res. J.*, 2004, **74**, 409–416.
29 X. Guo, W. Ouyang and B. Xu, Assessing cotton maturity using distributional parameters of fiber cross-section measurements, *Text. Res. J.*, 2014, **84**, 1666–1676.
30 C. A. Schneider, W. S. Rasband and K. W. Eliceiri, NIH Image to ImageJ: 25 years of image analysis, *Nat. Methods*, 2012, **9**, 671–675.
31 S. Nam, I. S. Baek, M. B. Hillyer, Z. He, J. Y. Barnaby, B. D. Condon and M. S. Kim, Thermosensitive textiles made from silver nanoparticle-filled brown cotton fibers, *Nanoscale Adv.*, 2022, **4**, 3725–3736.
32 S. Nam, M. B. Hillyer, Z. He, S. Chang and J. V. Edwards, Self-induced transformation of raw cotton to a nanostructured primary cell wall for a renewable antimicrobial surface, *Nanoscale Adv.*, 2022, **4**, 5404–5416.
33 S. Nam, G. W. Selling, M. B. Hillyer, B. D. Condon, M. S. Rahman and S. Chang, Brown cotton fibers self-produce Ag nanoparticles for regenerating their antimicrobial surfaces, *ACS Appl. Nano Mater.*, 2021, **12**, 13112–13122.
34 S. Nam, H. Tewolde, Z. He, K. Rajasekaran, J. Cary, G. Thyssen, H. Zhang, C. Sickler and M. M. Islam, Biodegradation Resistance of Cotton Fiber Doped with Interior and Exterior Silver Nanoparticles in Soil, *ACS Omega*, 2024, **9**, 13017–13027.
35 P. J. Wakelyn, N. R. Bertoniere, A. D. French, D. P. Thibodeaux, B. A. Triplett, M. Rousselle, W. R. J. Goynes, J. V. Edwards, L. Hunter, D. D. McAlister and G. R. Gamble, *Cotton Fiber Chemistry and Technology*, CRC Press, 2006.
36 M. Chen, T. T. Zhang, L. He, K. Wang and Y. Chen, Qualitative analysis of cotton fiber pigment composition, *Text. Res. J.*, 2021, **91**, 456–463.
37 M. Taniguchi, C. A. LaRocca, J. D. Bernat and J. S. Lindsey, Digital database of absorption spectra of diverse flavonoids enables structural comparisons and quantitative evaluations, *J. Nat. Prod.*, 2023, **28**, 1087–1119.
38 R. L. Long and M. P. Bange, Consequences of immature fiber on the processing performance of Upland cotton, *Field Crops Res.*, 2011, **121**, 401–407.
39 V. V. Salnikov, M. J. Grimson, R. W. Seagull and C. H. Haigler, Localization of sucrose synthase and callose in freeze-substituted secondary-wall-stage cotton fibers, *Protoplasma*, 2003, **221**, 175–184.
40 M. Song, D. Wang, S. Peana, S. Choudhury, P. Nyga, Z. A. Kudyshev, H. Yu, A. Boltasseva, V. M. Shalaev and A. V. Kildishev, Colors with plasmonic nanostructures: a full-spectrum review, *Appl. Phys. Rev.*, 2019, **6**, 041308.
41 T. M. Benn and P. Westerhoff, Nanoparticle silver released into water from commercially available sock fabrics, *Environ. Sci. Technol.*, 2008, **42**, 4133–4139.
42 C. Lorenz, L. Windler, N. von Goetz, R. P. Lehmann, M. Schuppler, K. Hungerbühler, M. Heuberger and B. Nowack, Characterization of silver release from

commercially available functional (nano)textiles, *Chemosphere*, 2012, **89**, 817–824.

43 L. Geranio, M. Heuberger and B. Nowack, The behavior of silver nano textiles during washing, *Environ. Sci. Technol.*, 2009, **43**, 8113–8118.

44 M. Gorjanc, V. Bukošek, M. Gorenšek and M. Mozetič, CF4 plasma and silver functionalized cotton, *Text. Res. J.*, 2010, **80**(20), 2204–2213.

45 D. Hegemann, M. M. Hossain and D. J. Balazs, Nanostructured plasma coatings to obtain multifunctional textile surfaces, *Prog. Org. Coat.*, 2007, **58**, 237–240.

46 S. Nourbakhsh, Antimicrobial performance of plasma corona modified cotton treated with silver nitrate, *Russ. J. Appl. Chem.*, 2018, **91**, 1338–1344.

47 S. Nam, S. E. Chavez, M. B. Hillyer, B. D. Condon, H. Shen and L. Sun, Interior *vs.* exterior incorporation of silver nanoparticles in cotton fiber and washing durability, *AATCC J. Res.*, 2021, **8**, 1–12.

48 S. Nam, M. B. Hillyer, B. D. Condon, J. S. Lum, M. N. Richards and Q. Zhang, Nanoparticle-infused cotton fiber: Durability and aqueous release of silver in laundry water, *J. Agric. Food Chem.*, 2020, **68**, 13231–13240.